

An HST Survey of the Disk Cluster Population of M31. II. ACS Pointings¹

O. K. KRIENKE
Seattle Pacific University, Seattle, WA okk@spu.edu

AND

P. W. HODGE
University of Washington, Seattle, WA hodge@astro.washintgon.edu

ABSTRACT. This paper reports on a survey of star clusters in M31 based on archival images from the *Hubble Space Telescope*. Paper I (Krienke and Hodge 2007) reported results from images obtained with the Wide Field/Planetary Camera 2 (WFPC2) and this paper reports results from the Advanced Camera for Surveys (ACS). The ACS survey has yielded a total of 339 star clusters, 52 of which, mostly globular clusters, were found to have been cataloged previously. As for the previous survey, the luminosity function of the clusters drops steeply for absolute magnitudes fainter than $M(V) = -3$; the implied cluster mass function has a turnover for masses less than a few hundred solar masses. The color-integrated magnitude diagram of clusters shows three significant features: (1) a group of very red, luminous objects: the globular clusters, (2) a wide range in color for the fainter clusters, representing a considerable range in age and reddening, and (3) a maximum density of clusters centered approximately at $V = 21$, $B - V = 0.30$, $V - I = 0.50$, where there are intermediate-age, intermediate-mass clusters with ages close to 500 million years and masses of about 2000 solar masses. We give a brief qualitative interpretation of the distribution of clusters in the CMDs in terms of their formation and destruction rates. (key words: star clusters and associations; galaxies)

1. INTRODUCTION

This is the second paper in a series of two that reports the results of the identification and photometry of star clusters in the disk of the galaxy M31 (NGC 224). Paper I (Krienke and Hodge 2007) presented details of a set of 343 clusters that were detected and measured on *Hubble Space Telescope* Wide Field Planetary Camera 2 images. The present paper reports on *HST* Advanced Camera for Surveys images.

¹ Based on observations with the NASA/ESA *Hubble Space Telescope* obtained at the Space Telescope Science Institute, which is operated by the Association of Universities for research in astronomy, Inc., under NASA contract NAS 5-26555.

A history of the searches for disk clusters in M31 was summarized in Paper I. Except for bright globular clusters, only a few young clusters in M31's disk had been studied in ground-based surveys. The crowding and the faint magnitudes required the characteristics of the *Hubble Space Telescope* to make reliable identifications and measurements. Several important recent papers, listed in Paper I, have dealt with unusually luminous young clusters ("blue globular clusters") based on HST images. However, previous work on traditional "open clusters" in M31 has been more limited. The most important recent paper published before our Paper I is that of Barmby and Huchra (2001), who identified 20 probable open clusters and showed HST images of them.

We note here that, as in Paper I, we adopt the following parameters for M31: distance: 725 kpc, position angle of major axis: 37 degrees, inclination angle: 12.5 degrees to the line-of-sight, mean foreground reddening: $E(B - V) = 0.20$, mean internal reddening: $E(B - V) = 1.0$. The internal reddening in the optical in M31 is highly variable because of the relatively high dust content and the small inclination angle. Our survey of galaxies seen through the M31 disk on the ACS images, which we hope to publish soon, indicates that the optical depth in some of our areas is highly-structured.

2. OBSERVATIONAL MATERIAL

For this survey we chose 27 pointings from the list (as of 1 January 2007) of ACS exposures included in the *HST* archives. We made the following requirements: (1) there should be at least two colors from the various HST filters that provide colors convertible to B, V or I, (2) the location should be in the main disk of M31, though we chose two outer pointings for comparison, (3) the exposures should be at least 400 seconds (with the exception of dataset j92ga7vlq, for which the F555W exposure was only 151 seconds) and (4) the star density should be such that clusters would not be swamped by field stars, as is the case in the inner bulge and the nucleus region. When there were several pointings in the same region, we chose representative selections. The total area scanned was $278.37 \text{ (arcmin)}^2$. Figure 1 shows the distribution of the chosen pointings on the disk of M31 and Table 1 lists the pointings, their positions, filters and exposures. Because of the fact that we were limited to archival data, with filters and exposures dictated by other considerations, the ACS sample is somewhat less uniform in characteristics than the WFPC2 sample.

We located and measured a total of 339 star clusters. The search techniques and measurement procedures for this program were identical to those of Paper I. Star clusters were identified independently by each of the authors using the criteria described in Paper I. Candidates were accepted only if the images were unambiguous in both colors. As in the first survey (Paper I), there was an approximately equal number of possible, but doubtful, clusters noted. They are not tabulated or discussed here, as their true nature will require further observational tests.

Positions, integrated magnitudes and colors were obtained for each cluster, as described in Paper I. The largest uncertainty in the photometry is caused by the variable background of the M31 disk, which contributes significantly to the measurements for

faint clusters. As in Paper I, for each cluster we measured the surface brightness and color of a large number of nearby background areas the same size as the adopted cluster size, allowing a determination of the background and its uncertainty. The colors and magnitudes were converted from the observed filters and exposures to standard B, V, and I values by using the method given by Siriani et al. (2002). Table 2 lists the mean measurement errors as a function of cluster integrated magnitude and color.

Comparing our data with previous catalogs, primarily the Revised Bologna Catalog of Clusters in M31 (hereafter, RBC) (Galleti et al. 2004) and the more recent list of new discoveries by Kim et al. (2007), we find that there are 52 clusters in common, most of them classified as globular clusters. Nine of them are rediscoveries of open clusters first observed by Hodge (1979). Table 3 lists the previously cataloged clusters and provides our photometry for them. Average differences in the sense of our values minus the RBC values are as follows: $\Delta V = 0.25 \pm 0.08$, $\Delta B = 0.10 \pm 0.07$, $\Delta I = 0.26 \pm 0.12$. We point out that these values are all positive, which is likely the result our use of small apertures to minimize the effects of the background on cluster colors. Some of the differences may also be the result of the fact that some of the RBC measurements come from older photographic values.

Table 4, which in its entirety is available in the electronic edition of the Publications, lists all of the new clusters, their positions, their integrated magnitudes and their colors. We have continued the numbering of clusters from Paper I; thus, the first of the new clusters is named KHM31-284.

Figure 2 shows a sampling of clusters, illustrating the range in size, structure, and brightness of the sample.

3. CLUSTER PROPERTIES

3.1. The luminosity Function

The observed luminosity function for the new clusters listed in both this paper and Paper I is shown in Figure 3. There is a dearth of bright globular clusters, as they had already been cataloged. The distribution shows a turn-over at an absolute magnitude of approximately $M(V) = -3.0$. It should be noted that the derived luminosity function may be biased by the fact that there is a range of exposure times in our sample. However, our tests of cluster detectability for images with different exposure times do not show a correlation. Apparently the number of clusters detected is more influenced by intrinsic and extrinsic effects (formation rates, extinction, etc.) than by exposure time.

3.2 Color-Magnitude Diagrams

In Figure 4 we plot the observed integrated magnitudes and colors for the two ACS samples, those with B and V colors and those with V and I. These diagrams have very similar distributions of points to those found for the sample of clusters in Paper I. There are three interesting features of all of these color-magnitude diagrams (CMDs):

1. the colors show a wide range of values, suggesting the presence of clusters of many ages, though the large uncertainties of colors for the faintest clusters weakens this conclusion for them.
2. there are a few very luminous, red clusters that stand out from the rest. These are the traditional globular clusters.
3. the fainter (“open”) clusters show a distribution with a maximum density in the middle part of the diagram, where the typical intermediate-age, intermediate-mass clusters with ages close to 500 million years and masses of about 2000 solar masses (Girardi 2006). We interpret this concentration to be the result of an approximately constant rate of cluster formation plus reddening of clusters with age. This would predict few very blue (young) clusters and few very red ones (because of aging or disruption). We have discussed both of these effects in Paper I and the new results are in agreement with those presented there.

We note that our CMD for clusters shows a very different distribution from that of a CMD for a typical sampling of stars in the M31 disk (e.g., Magnier et al. 1997 and Williams 2003), which shows a more evenly-spread distribution of points, without the bunching of points at intermediate colors exhibited by the clusters. As explained above, this is the result of the fact that the clusters concentrate stars of a limited range of ages, because of dynamical evolution, so that the age distribution of clusters is skewed compared to that of field stars.

These CMDs plot the observed colors and magnitudes, uncorrected for reddening. The reddening correction for these clusters cannot be measured with existing data, as we have only two colors available for all but three of the pointings, and, in any case, the large variations in the background would make the uncertainties in colors too large for precise reddening determinations.

4. THE SPATIAL DISTRIBUTION

Figure 5 shows the distribution of the cluster density (corrected to face-on) in the disk as a function of distance from the center. We have combined the data with that of Paper I and have removed the globular clusters from this diagram, assuming them to belong to a different dynamical system. The diagram shows a relative paucity of clusters within 5 kpc (although the number of fields sampled there is small), a maximum density in the range 8 to 15 kpc and a gradual decrease beyond 15 kpc. Also, as for the sample of Paper I, the cluster density is correlated with the distance from the nearest star-forming region.

5. CONCLUSION

These two surveys of M31, using two cameras of the *Hubble Space Telescope*, have shown that the disk of M31 contains a large number of star clusters with a wide range of observable properties (luminosity, size, color) and a wide range of implied characteristics

(mass, age, dynamical history). The total area scanned for clusters in the two papers is 477.4 (arcmin)^2 , which is 4.9% of the area of the disk (depending on how the disk's boundaries are defined). The implied total number of disk clusters is on the order of 10^4 , indicating that the clusters offer a rich vein of material for the study of the history and mechanisms of star and cluster formation and destruction. To mine this vein will require accurate measurements of individual clusters' reddenings and extinction. We have begun a program that examines several methods of accomplishing this with existing data.

We are indebted to the American Astronomical Society's Small Grant Program for publication funds and to NASA and the Space Telescope Science Institute for making the archival images available.

References

- Barmby, P. and Huchra, J. 2001, AJ, 122, 2458
- Ferguson, Annette M. N.; Irwin, Michael J.; Ibata, Rodrigo A.; Lewis, Geraint F.; Tanvir, Nial R. 2002, AJ 124, 1452
- Galleti, S., Federici, L., Bellazini, M., Fusi Pecci, F. & Macrina, S. 2004, A&A, 416, 917
- Girardi, L. 2006, <http://pleiadi.pd.astro.it>
- Hodge, P. W. 1979, AJ, 84, 744
- Kim, S. C., Lee, M G., Geisler, D., Sarajedini, A., Park, H. S., Hwang, H. S., Harris, W. E., Seguel, J. C., von Hippel, T. 2007, AJ, 134, 706
- Krienke, O. K. and Hodge, P. W. 2007, PASP, 119, 7
- Magnier, E., Hodge, P. W. Battinelli, P., Lewin, W. and van Paradijs, J. 1997, MNRAS, 292, 490
- Sirianni, M., De Marchi, G., Gilliland, R., Jee, M. K., Mack, J., Ford, H. C., Illingworth, G. D., Clampin, M., Hartig, G., Cross, N., STScI ACS Team, 2003, BAAS, 35, 722
- Williams, B. F. 2003, AJ, 126, 1312

Figure Captions

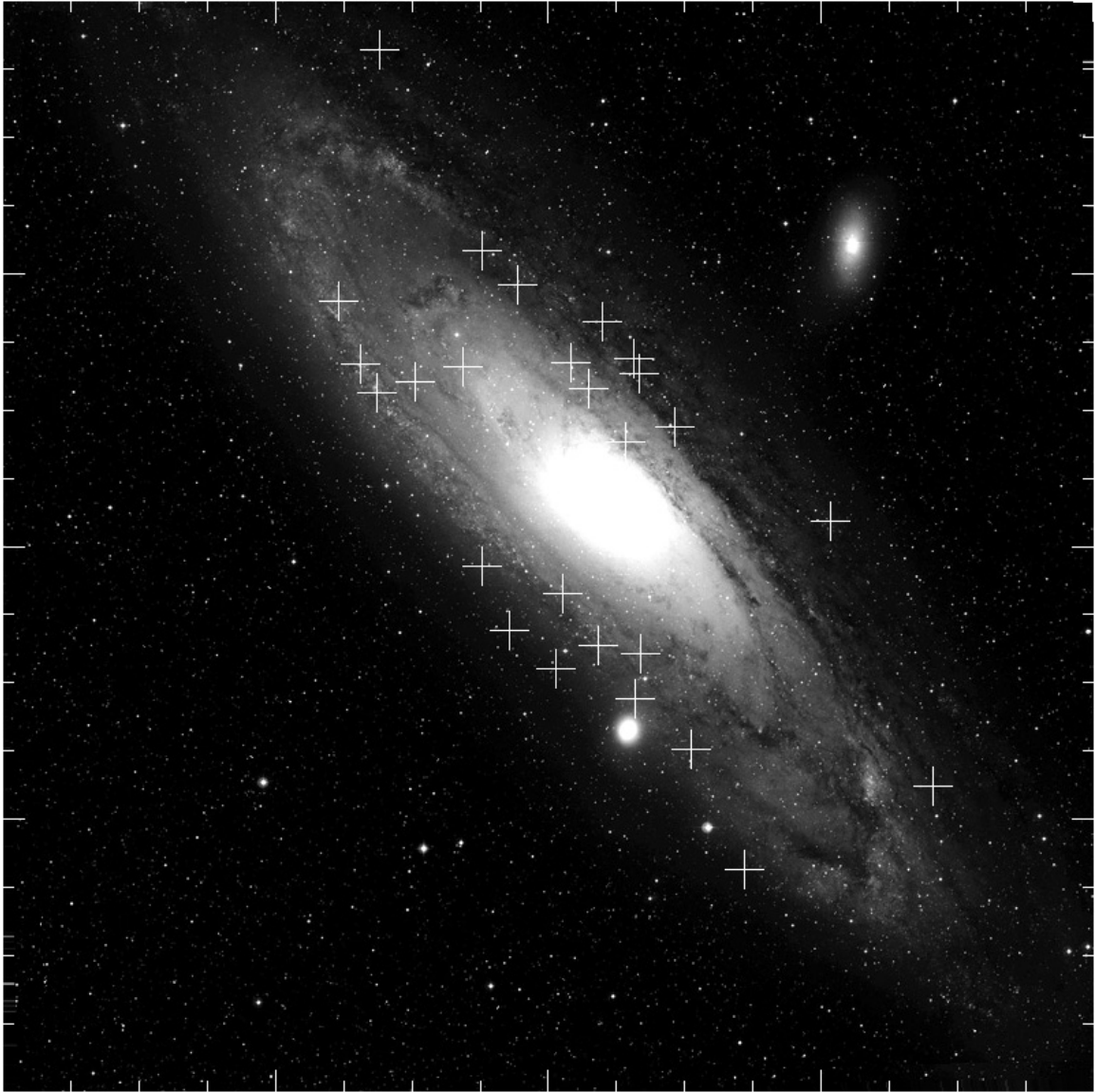


FIG. 1. – The locations of the *HST* ACS pointings that were used to search for star clusters. The background photograph is as described in Paper I. Two outer fields are beyond the edges of the figure (see Table 1). The width of the image is 85 minutes of arc. Note that the symbols are larger than the size of the ACS fields.

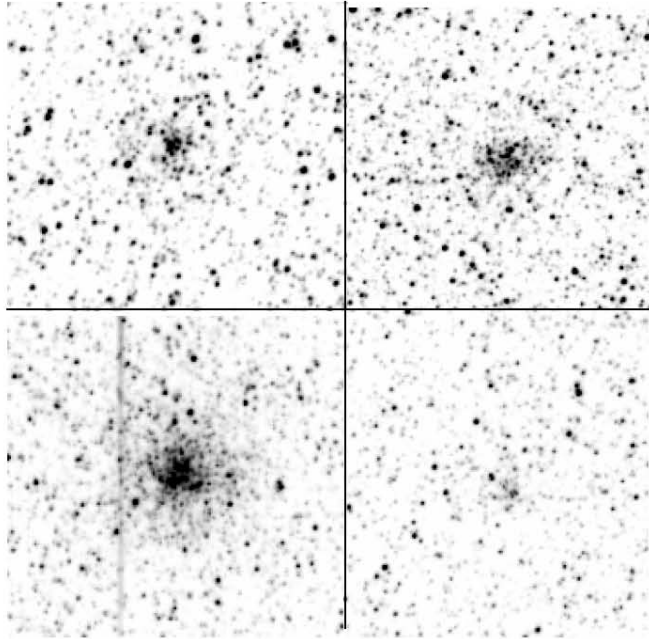


FIG. 2. – Four sample disk clusters. The upper left image is of KHM31-538 with an integrated magnitude of $V = 20.97$. The upper right cluster is KHM31-399, with $V = 21.08$. The lower left cluster, one of the brightest, is KHM31-409, with $V = 18.87$. The vertical streak is caused by a very luminous star directly above the field. The lower right panel shows one of the faintest clusters, KHM31-395, with $V = 22.64$. Each image is 17.5 arc seconds wide.

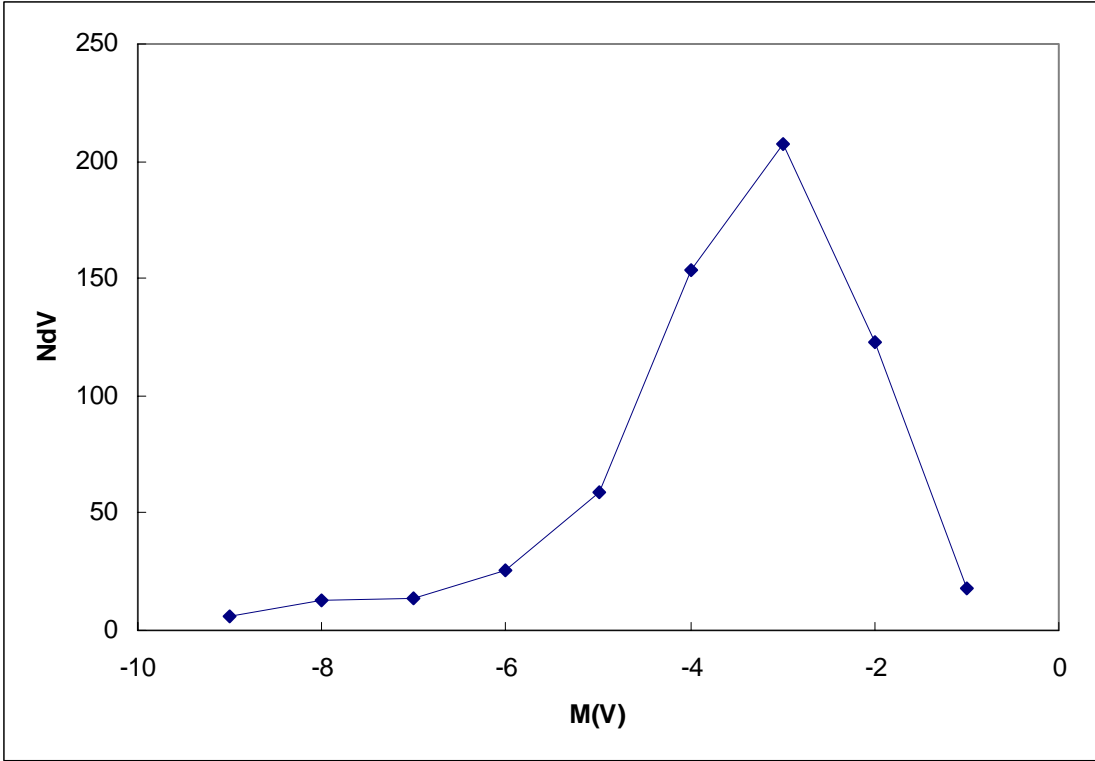
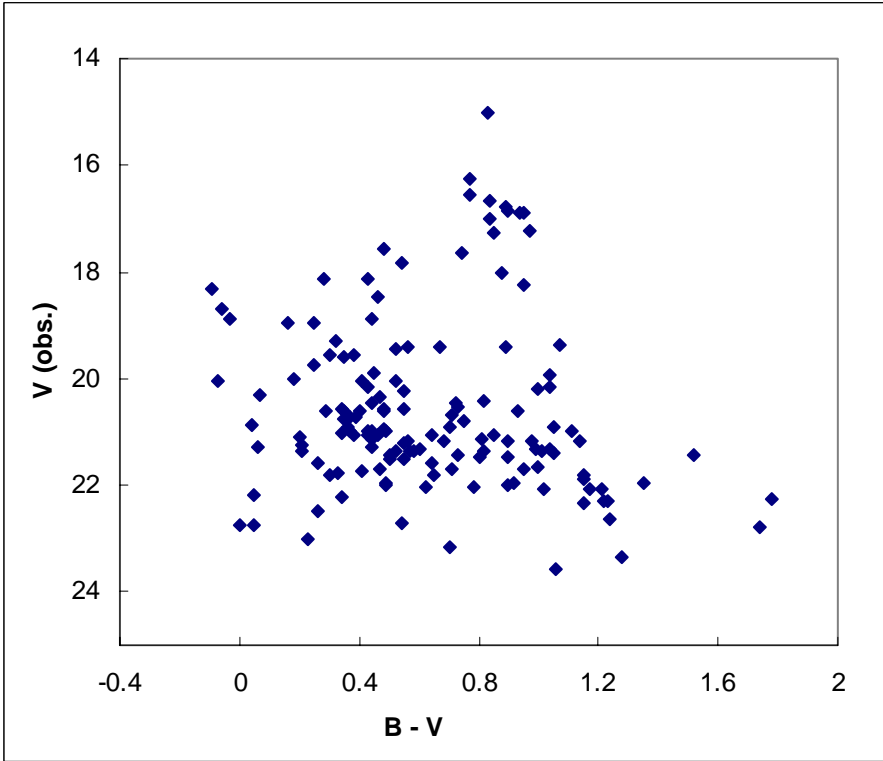


FIG. 3. – Integrated luminosity function of the new clusters measured in Paper I and this paper. The dots are connected by straight lines for clarity.



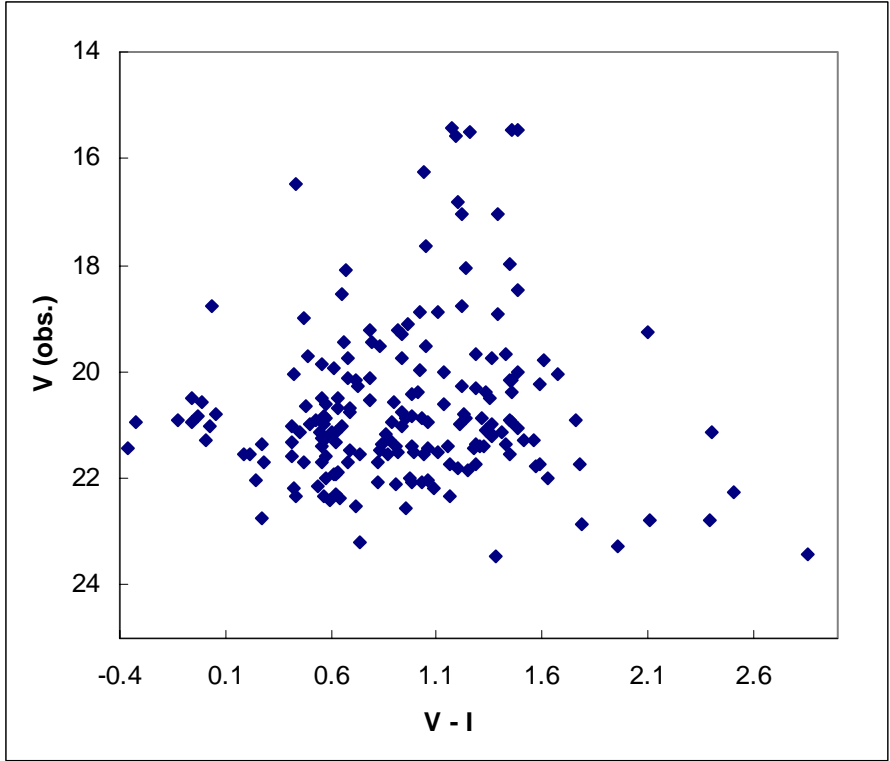


FIG. 4. – Integrated color-magnitude diagrams for all clusters detected in the ACS survey (Tables 2 and 3). The globular clusters occupy the upper right-hand area of the arrays.

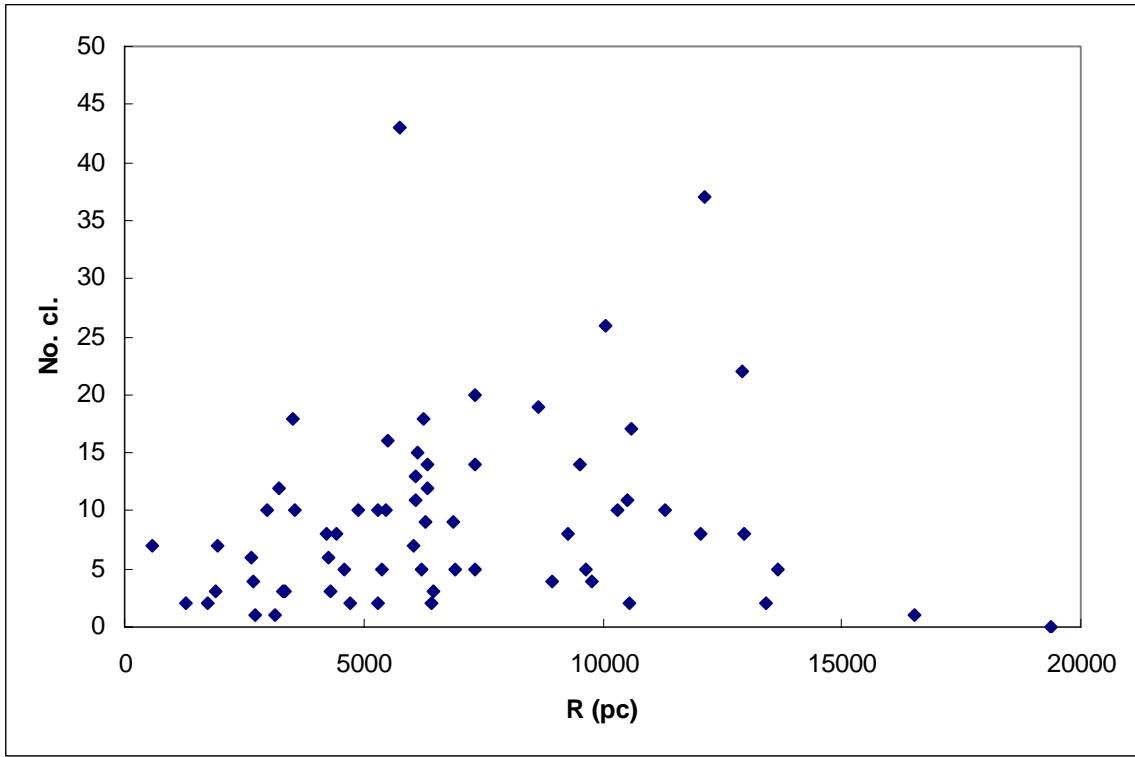


FIG. 5. – The radial distribution of clusters in the survey. We plot the number of clusters per field as a function of distance from the M31 nucleus, assuming all to be in the plane.

Tables

TABLE 1
HST ACS POINTINGS SEARCHED

Dataset	RA	Dec	Ncom- bine	Filter 1	Filter 2	Exp 1	Exp 2
j8mg01071	9.884423	40.78762	3	F555W	F814W	870	825
j96q07010	10.12638	41.25184	4	F606W	F435W	3250	7260
j8mg04071	10.32099	40.64206	3	F555W	F435W	825	1200
J96Q06010	10.44707	40.85222	3	F606W	F435W	2110	2672
j92gb1d3q	10.49058	41.41872	1	F555W	F814W	413	502
j8z004010	10.56584	41.02121	3	F606W	F814W	2370	2370
j92gb2hyq	10.5765	41.51019	1	F555W	F814W	413	502
j92gb9brq	10.57663	40.94247	1	F555W	F814W	413	800
j8z007010	10.5878	41.53735	3	F606W	F814W	2370	2370
J92GB5NFQ	10.60658	41.39225	1	F555W	F814W	413	502
j92gb3dpq	10.66242	41.60167	1	F555W	F814W	413	502
j92gb0cuq	10.66254	41.03394	1	F555W	F814W	413	502
J92GB6ZNQ	10.6925	41.48375	1	F555W	F814W	413	502
j92ga7vlq	10.73546	41.52947	1	F555W	F814W	151	457
J92GB4E9Q	10.74833	41.69314	1	F555W	F814W	413	502
J92GD1FPQ	10.74846	41.12542	1	F555W	F814W	413	502
j92gd4q4q	10.76183	40.99308	1	F555W	F814W	413	502
j92gb8vyq	10.86433	41.66669	1	F555W	F814W	413	502
j8f102cxq	10.86938	41.06218	1	F606W	F814W	1000	1580
J92GD6D5Q	10.93575	41.17469	1	F555W	F814W	413	502
j8mg08071	10.94756	41.72721	3	F555W	F814W	825	1200
j96q05010	10.9882	41.52269	3	F606W	F435W	1840	2925
j96q02010	11.10045	41.4973	3	F606W	F435W	1860	2910
j96q04010	11.18791	41.47789	3	F606W	F435W	3315	4560
j96q01010	11.19553	42.07823	3	F606W	F435W	1850	2920
j8o440071	11.22637	41.52669	2	F606W	F814W	1830	1548
j8mg07071	11.28035	41.63718	3	F555W	F435W	825	1200

TABLE 2

MEAN MEASUREMENT ERRORS
AS A FUNCTION OF MAGNITUDE AND COLOR

V	Verr	(B - V)err	(V - I)err
15	0.01	0.01	0.32
16	0.03	0.05	0.03
17	0.03	0.04	0.18
18	0.04	0.07	0.28
19	0.06	0.06	0.24
20	0.11	0.12	0.22
21	0.12	0.14	0.22
22	0.23	0.39	0.23
23	0.21	0.32	0.23

TABLE 3
CLUSTERS PREVIOUSLY IDENTIFIED

Name	RA	Dec	V	Verr	B	Berr	B-V	I	Ierr	V - I
B008	10.12540	41.26899	17.00	0.04	17.83	0.03	0.84			
B010	10.13076	41.23949	16.65	0.01	17.49	0.01	0.84			
c136	10.31879	40.65087	18.96	0.04	19.21	0.05	0.25			
c137	10.32659	40.65050	19.54	0.18	19.92	0.10	0.38			
I-34	10.42351	40.86716	19.41	0.06	20.08	0.04	0.67			
B031D	10.43581	40.85639	18.46	0.04	18.92	0.04	0.46			
B049	10.43972	40.83202	17.83	0.03	18.37	0.03	0.54			
I-36	10.44723	40.85249	20.16	0.07	21.20	0.08	1.04			
B253	10.45694	40.88346	19.42	0.03	19.98	0.04	0.56			
B057	10.46986	40.86823	17.65	0.02	18.40	0.02	0.74			
B069	10.52268	41.43591	18.56	0.05				17.91	0.09	0.65
BO82	10.56578	41.02058	15.54	0.01				13.65	0.01	1.89
c200	10.57332	40.92097	19.22	0.09				18.30	0.07	0.92
B088	10.58760	41.53736	15.47	0.01				14.01	0.01	1.46
B091	10.59064	41.36819	18.09	0.04				17.42	0.05	0.67
B093	10.59661	41.36217	16.82	0.05				15.63	0.05	1.20
B094	10.60413	40.95485	15.59	0.01				14.39	0.01	1.19
B056D	10.61819	41.57427	18.92	0.03				17.53	0.04	1.39
B067D	10.66196	41.61187	19.29	0.06				18.35	0.10	0.94

c232	10.66636	41.03948	20.86	0.35					19.92	0.29	0.95
B130	10.70352	41.49801	17.05	0.03					15.66	0.02	1.39
B137	10.72515	41.53742	17.99	0.04					16.54	0.04	1.45
II-113	10.72948	40.99620	19.23	0.06					18.45	0.10	0.78
B140	10.74456	41.14800	18.06	0.04					16.82	0.04	1.24
B087D	10.74525	41.15242	17.64	0.02					16.59	0.03	1.05
B141	10.74725	41.54663	17.03	0.02					15.81	0.02	1.22
B091D	10.75618	41.50491	15.44	0.02					14.27	0.02	1.17
B266	10.76432	41.67529	18.48	0.03					17.00	0.01	1.48
B174	10.87643	41.64898	15.52	0.01					14.26	0.01	1.26
I-66	10.85047	41.64513	20.37	0.13					19.04	0.12	1.33
c259	10.89531	41.16478	16.48	0.06					16.05	0.09	0.43
B198	10.95866	41.53125	18.01	0.05	18.89	0.09	0.88				
I-74	10.95903	41.69659	19.50	0.04					18.45	0.06	1.05
B201	10.97008	41.16607	16.24	0.03					15.20	0.03	1.04
B203	10.98252	41.54302	16.79	0.02	17.68	0.02	0.89				
B206	10.99418	41.50498	15.02	0.01	15.85	0.01	0.83				
B213	11.01455	41.51070	16.89	0.00	17.84	0.06	0.95				
B215	11.02659	41.52876	17.24	0.02	18.22	0.02	0.97				
B220	11.08072	41.50987	16.54	0.01	17.31	0.02	0.77				
BO224	11.11256	41.48057	15.23	0.01	15.99	0.01	0.76				
M047	11.15783	41.48106	19.42	0.05	20.30	0.05	0.89				
B231	11.16090	41.46298	17.28	0.02	18.13	0.03	0.85				
B234	11.19340	41.48818	16.85	0.02	17.76	0.03	0.90				
B366	11.19428	42.06411	16.27	0.03	17.04	0.04	0.77				
B367	11.19632	42.09233	18.13	0.03	18.56	0.02	0.43				
B255D	11.20214	42.10382	18.25	0.07	19.19	0.06	0.95				
c406	11.21377	41.49024	20.30	0.04	20.37	0.03	0.03				
III-159	11.22247	41.53220	20.40	0.08					19.39	0.10	1.01
c305	11.25343	41.51674	18.98	0.18					18.51	0.08	0.47
c311	11.29325	41.61290	18.32	0.06	18.23	0.05	0.09				
c312	11.29936	41.62017	18.14	0.10	0.08	0.01	0.28				
c313	11.30592	41.62668	17.58	0.02	18.05	0.02	0.48				

NOTE: The cluster names are from the RBC (Galleti et al 2004), except for names prefixed by I, II, and III which are from the three tables in Kim et al (2007) and those prefixed by c, which are from Hodge (1979)

TABLE 4
NEW STAR CLUSTERS

Name	RA	Dec	V	Verr	B	Berr	B-V	I	Ierr	V-I
------	----	-----	---	------	---	------	-----	---	------	-----

KHM31-284	9.89001	40.77265	21.75	0.22				20.16	0.31	1.59
KHM31-285	9.89011	40.77258	21.76	0.16				20.19	0.16	1.57
KHM31-286	9.89566	40.81459	22.28	0.29				21.66	0.21	0.62
KHM31-287	9.92680	40.77808	22.77	0.14				20.66	0.11	2.11
KHM31-288	10.10328	41.24350	23.16	0.27	23.87	0.27	0.70			
KHM31-289	10.10461	41.25509	21.87	0.19	23.02	0.20	1.15			
KHM31-290	10.13054	41.22922	21.12	0.10	21.93	0.11	0.81			
KHM31-291	10.16101	41.26554	20.43	0.08	21.25	0.08	0.82			
KHM31-292	10.29633	40.64710	21.44	0.09	22.17	0.11	0.73			
KHM31-293	10.29917	40.63040	21.07	0.15	21.50	0.12	0.43			

NOTE. – Table 4 is published in its entirety in the electronic edition of the *PASP*. A portion is shown here for guidance regarding its form and content.